COBEM 2023 27TH INTERNATIONAL CONGRESS OF MECHANICAL ENGENEERING

ABCM Brazilian Society of Mechanical Sciences and Engineering
27th ABCM International Congress of Mechanical Engineering
December 04-08, 2023, Florianópolis-SC, Brazil

COB-2023-2133
COMBUSTION SIMULATION OF A PARAFFIN BASED SOLID FUEL WITH GASEOUS OXYGEN INSIDE A HYBRID ROCKET MOTOR

Paulo Gabriel Cunha Martins
Rene Gonçalves
Leonardo Henrique Gouvêa
Cristiane Aparecida Martins
Aeronautics Institute of Technology
paulomartins92@gmail.com
renefbg@ita.br
gouvea@ita.br
cmartins@ita.br

Abstract. *For the last two decades, the hybrid rocket propulsion community has researched paraffin-based fuels because it offers high values of regression rate compared to traditional fuels commonly used, such as hydroxyl-terminated polybutadiene or polyethylene. However, Paraffin does not have good mechanical properties, which increases the risk of grain cracking and rupturing. This work presents a simulation performed at ANSYS Fluent of the combustion process of a 100 newtons lab-scale hybrid rocket motor present in LPL ITA. The propellants of this hybrid rocket motor are paraffin wax and gaseous oxygen. The simulations utilize a mesh with around 100000 quadrilaterals elements, with an average orthogonal quality of 96.5% and an average skewness of 1%. The volume domain of the simulations is axis-symmetric. Paraffin is studied as hexadecane ($C_{16}H_{34}$) using a reduced reaction mechanism of diesel from "Creck-modeling" at the gas phase. The simulations are at a steady state at different periods during the propulsion. Three simulations are present at times of 0, 5, and 10 of the hybrid rocket motor operation. The results analyzed are temperature, pressure, velocity, and some species profiles inside the hybrid rocket motor. The nozzle and the plume of the exhaust product gases are also present. The results did contribute to the understanding of the burning process during tests. The simulations did help during the project of a lab-scale hybrid rocket motor, which now operates with paraffin wax and other paraffin-based blends with gaseous oxygen.*

Keywords: *Hybrid rocket motor, Combustion simulation, Paraffin and gaseous oxygen, k-ω SST turbulence model, Nozzle analysis*

1. INTRODUCTION

This work aims to simulate the operation of a HRM (hybrid rocket motor) of 100 N that operates with Paraffin and gaseous oxygen as propellants. This simulation was performed during the project development of an HRM, designed by Martins (2018), that nowadays is active at LPL (Liquid propulsion laboratory) in ITA (Aeronautics Institute of Technology) Martins *et al.* (2023). The numerical simulation was developed to validate the results obtained analytically during the design and to calculate the physicochemical properties of the propellant in each portion of the motor considering the geometry details inside the HRM. The flow behavior inside the combustion chamber and nozzle was obtained through numerical simulation using the software ANSYS Fluent ® and it was explained in the "Computational procedures" section.

In the section "Analytical procedures", the preliminary steps to design the hybrid rocket motor are explained among them thermodynamic analysis, regression rate analysis, and temporal analysis. The thermodynamic analysis determined the proportion of gaseous oxygen to paraffin using the program NASA CEA (Chemical Equilibrium Applications) from Gordon and J. McBride (1994) which calculated all the thermodynamic properties of the mixture for a given O/F (oxidizer to fuel ratio). The next step analyzed the regression rate of Paraffin resulting in the O/F over time of HRM operation as the main result. The temporal analysis interpolated the results from the latter analysis with the thermodynamic analysis resulting in the complete definition of HRM operation, also obtaining the internal ballistics geometry and theoretical performance of the hybrid rocket motor at the end.

In the section on "Computational procedures," the methodology of simulation is briefly explained, including the choice of turbulence model and combustion reaction model, the configurations of spatial discretization for the equations, the control volume with the boundary conditions, and the mesh. Past simulations that contributed to the configurations of this one presented here are available at Martins and Shynkarenko (2017); Martins *et al.* (2019, 2022). In the final section, the results for pressure, temperature, and velocity over time are presented. Contours on the control volume of simulation and the area-weighted average of the same properties along the convergent and divergent parts of the nozzle are presented.

The results showed a fast pressure drop over time inside the combustion chamber, somewhat unrealistic, however, showed that the nozzle is approximately adapted over time resulting in high propulsive efficiency.

2. ANALYTICAL PROCEDURES

During the project development of the hybrid rocket motor of 100 newtons, some preliminary analyses were performed in order to define the internal ballistics of the HRM, such as thermodynamic analysis using the program NASA CEA from Gordon and J. McBride (1994), regression rate analysis, and temporal studies of propulsive performance.

The regression rate analysis and the temporal studies of propulsive performance are the focus of this analytical part because the results here are input into the computational procedures presented in the next section. Regression rate analysis regards the mean rate that the fuel paraffin burns with gaseous oxygen. In hybrid rocket propulsion, researchers have found it suitable for the purpose of quantifying the burning rate of the propellant the following simplified expression, Humble *et al.* (1995).

$$\dot{r} = aG_{ox}^{n} \tag{1}$$

$$G_{ox} = \frac{\dot{m}_{ox}}{\pi r^2} \tag{2}$$

$\dot{r}$ = space-time averaged regression rate (m/s), a = regression-rate coefficient, n = regression-rate exponent and G_{ox} = oxidizer mass flux rate through port area (kg/m^2s), and m_{ox} = oxidizer mass flow rate (g/s).

The coefficients a and n are determined directly experimentally and depend on the propellants, grain configuration, and the type of injector used. Attention must be given to the G_{ox} range evaluated experimentally since the coefficients a and n are only true within the limits. For Paraffin and Gaseous oxygen in the range of 15 to 105 of G_{ox} the space-time averaged regression rates law chosen for this simulation corresponds to the paraffin-based fuel (SP-1) tested at Stanford university by Karabeyoglu *et al.* (2001), and is given by the following equation:

$$\dot{r} = 0.091G_{ox}^{0.69} \tag{3}$$

The temporal studies of propulsive performance consist of the interpolation over time of the regression rate equation 3. One can integrate the equation analytically or numerically. Integrating it results in the following equation 4.

$$r(t) = \left((a\,(2n+1)\,t) \left(10^3 m_{ox}/\pi \right)^n + r(t_0)^{2n+1} \right)^{1/(2n+1)} \tag{4}$$

$r(t)$ is in (mm), $r(t_0)$ is the port radius initially, and it was considered $r(t_0)$ constant equal to 10 mm. Knowing the port radius over time and the regression rate over time, the mass flow rate of fuel (paraffin) was calculated, and the oxidant to fuel ratio over time using the following equations.

$$\dot{m}_f(t) = 2\pi r(t) L \rho_f \dot{r}(t) \tag{5}$$

$$O/F = \frac{\dot{m}_f}{\dot{m}_{ox}} \tag{6}$$

During the design phase of the HRM, an O/F around 2.1 was desirable because it delivers high values of characteristic velocity, which is a property related to the combustion efficiency of the propellants. To achieve those values it was chosen a $\dot{m}_{ox}$ of 32 g/s. Density ρ_f of paraffin was considered equal to 920 kg/m^3. The length of the fuel grain of the HRM (L) measures 160 mm, and it was considered constant during burning.

Figure 1 shows the results of port radius, regression rate, the mass flow rate of paraffin, and O/F over time for a simulation of 10 s, using the above equations and constants. With red markers, there is the averaged time-and-space port radius of paraffin. At the initial time, the port radius is 10 mm, at the time 5 s port radius is 17 mm, and at the time 10 s port radius is approximately 21 mm. The results of port radius were considered as inputs in the simulations presented in the next section.

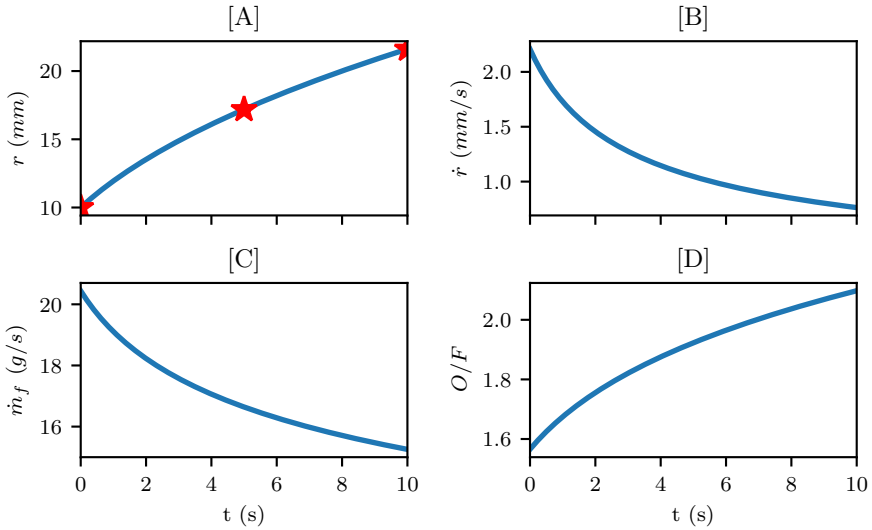

Figure 1. [A] radius, [B] regression rate, [C] fuel mass flow rate, and [D] O/F ratio varying along the burning time.

3. COMPUTATIONAL PROCEDURES

The numerical simulation was performed with commercial software fluent from ANSYS. The RANS (Reynolds-averaged Navier–Stokes) equations for single-phase multicomponent turbulent reacting flows were solved with a control volume-based technique and a pressure-based algorithm.

The stationary Navier-Stokes equations were supported by the $k-\omega$ SST (Shear Stress Transport) turbulent model. The $k-\omega$ SST turbulence model was created by Menter (1994) and it was chosen for the simulations because it is a low Reynolds model and has two functions: near the wall, it calculates the properties of the fluid more precisely using the standard k-ω model from Wilcox (1993), and in the core of the fluid, it uses the k-ϵ model from Jones, W P; Launder (1972), which results in the best performance of both models. This model is well presented in ANSYS manual Ansys (2006a),Ansys (2006b),Ansys (2006c) and in the article Martino *et al.* (2019).

The reduced diesel combustion model available on Stagni *et al.* (2015) calculated the species reactions inside the hybrid rocket motor. This reaction mechanism has 201 species with 4240 reactions, among them $C_{16}H_{34}$ and O_2 considered both in the gaseous phase as Paraffin and injector inlets. The species were modeled considering non-premixed combustion with steady diffusion flamelet since the simulation is in steady-state and chemical equilibrium could lead to unrealistic results, the energy treatment was non-adiabatic and the compressibility effects were as well considered.

Regarding the solution methods, the simulation was solved with a pressure-velocity coupled scheme, with a Rhie-Chow flux type. The spatial discretization was considered second order for pressure, density, momentum, turbulent kinetic energy, specific dissipation rate, energy, mean mixture fraction, and mixture fraction variance.

Figure 2 shows the two-dimensional control volume of the simulation. The simulation was treated as 2D axisymmetric to simplify the numerical calculations. However, the oxidizer injection was not properly modeled because it isn't axisymmetric, but the results obtained in the pre-chamber are still a suitable approximation.

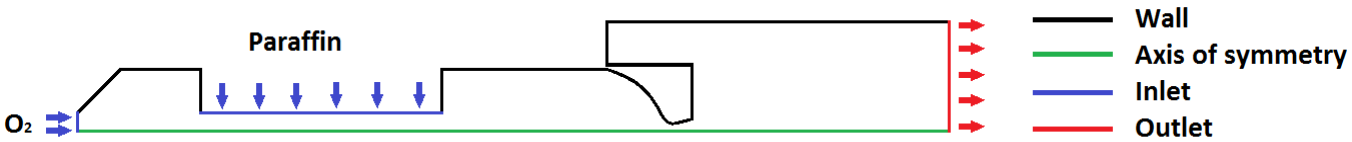

Figure 2. Boundary faces of the combustion chamber and nozzle.

In color blue are the injectors with a constant mass flow rate of gaseous O_2 and paraffin treated as gaseous $C_{16}H_{34}$. In black color is the solid wall with the non-slipping shear condition and adiabatic, in green is the axis of symmetry for rotation of the surfaces described and in red color is the pressure outlet with ambient pressure and the environment downstream the nozzle is considered as pure O_2 instead of air because is not possible to deal with more than two species in the simulation.

The parameters of the combustion chamber port radius and mass fluxes of paraffin over time considered for the simulations were calculated in the analytical studies, Figure 1, at 0, 5, and 10 seconds during the firing test. This simulation was designed to visualize the quantities of the properties, such as pressure, temperature, and velocity when this

hybrid motor is working on the test stand, disregarding the effects of gravity.

Figure 3 shows one of the meshes for this simulation, and it consists of around 100000 elements. Its distribution has a higher density near the walls to satisfy the $k-\omega$ turbulence model that requires $y^+ \simeq 1$ and enough nodal points (> 10) within the buffer region and sub-layers to detail the boundary layer. The present mesh presents y^+ between 0.5 and 15 inside the combustion chamber. Thanks to the work of Esch and Menter (2003), in the current software (ANSYS Fluent, CFX), the $k-\omega$ *SST* turbulence model uses a hybrid function that uses or does not uses the wall functions depending on the value of y^+. In locations where $y^+ > 1$, the wall functions are automatically activated, thus allowing the use of this turbulence model with a less refined mesh without losing the quality of the results, as can be observed in the paper of Menter *et al.* (2003).

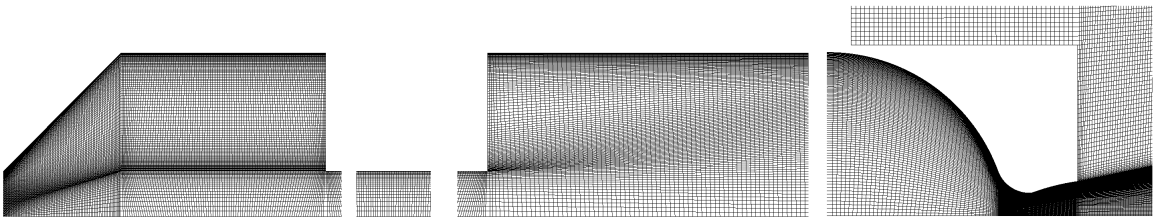

Figure 3. Distribution of the elements in the mesh over all the control volume and near the wall.

The model FLUID81 implemented in ANSYS Fluent® was used to generate this mesh. This model was considered to be appropriate for the axisymmetric simulations of fluids inside pipes, where the variation of pressure and temperature influence the structure of the turbulences and the interaction between wall and fluid, ANSYS (2009).

4. RESULTS

The criterion of results convergence considered was the residuals values of each simulation. It was considered that, when the residuals of energy were below the limits of 10^{-4} and the corresponding values of continuity, x-velocity, y-velocity, k, omega, fmean, and fvar were stabilized, the solution had converged and the results were determined.

The results obtained in this simulation were the pressure, temperature, and velocity inside the HRM and nozzle. The contour of absolute pressure is present in Figure 4. The values inside the hybrid rocket motor distinguish a little, representing a pressure damping over time. The exact value for static pressure inside the combustion chamber is presented later in Figure 7.

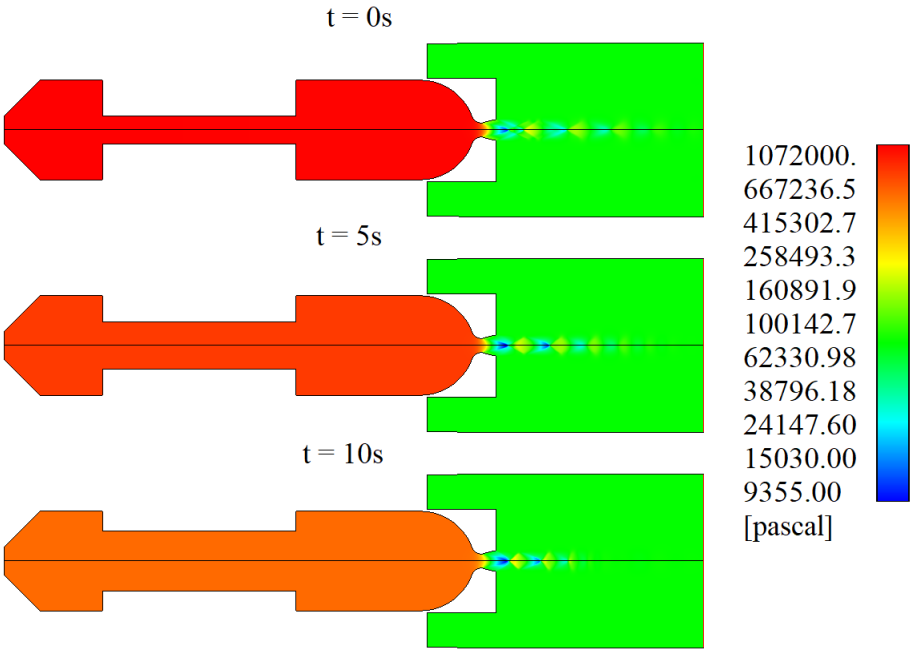

Figure 4. Pressure distribution on the control volume.

In Figure 5 are presented the values of the temperature inside the HRM. The results in the pre-chamber for any property can't be believed since the injector wasn't well described by the axisymmetric simulation, but it is a good initial step. The

values of temperature increase in the pre-chamber and decrease through the combustion chamber port, post-combustion chamber, and nozzle.

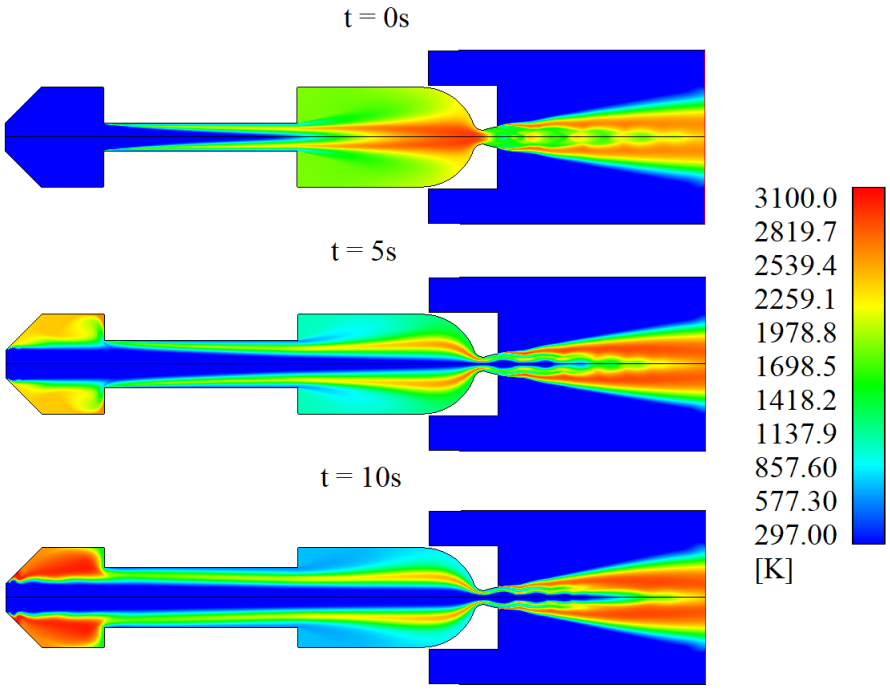

Figure 5. Temperature distribution on the control volume.

Figure 6 presents the distribution of velocity inside the HRM. The velocity from the pre-chamber up to the convergent part of the nozzle is in a subsonic regime. In the throat, the mixture reaches Mach 1, and on the divergent part, the flow reaches supersonic velocity.

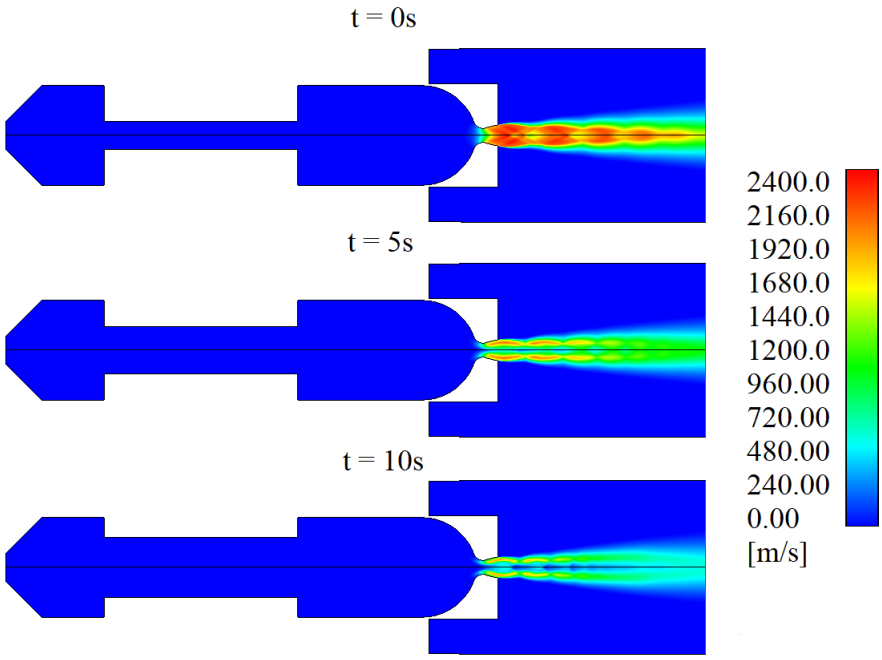

Figure 6. Velocity distribution on the control volume.

The area-weighted average of the properties pressure, temperature, and Mach number along the convergent and divergent part of the nozzle was calculated. Those values obtained for each simulation were compared with each other and are presented in Figure 7.

The observed values in the last results are better assessed through Figure 7. Over time all the values decrease at some point towards the nozzle exit. The pressure and temperature damping in the combustion chamber are due to the growth of

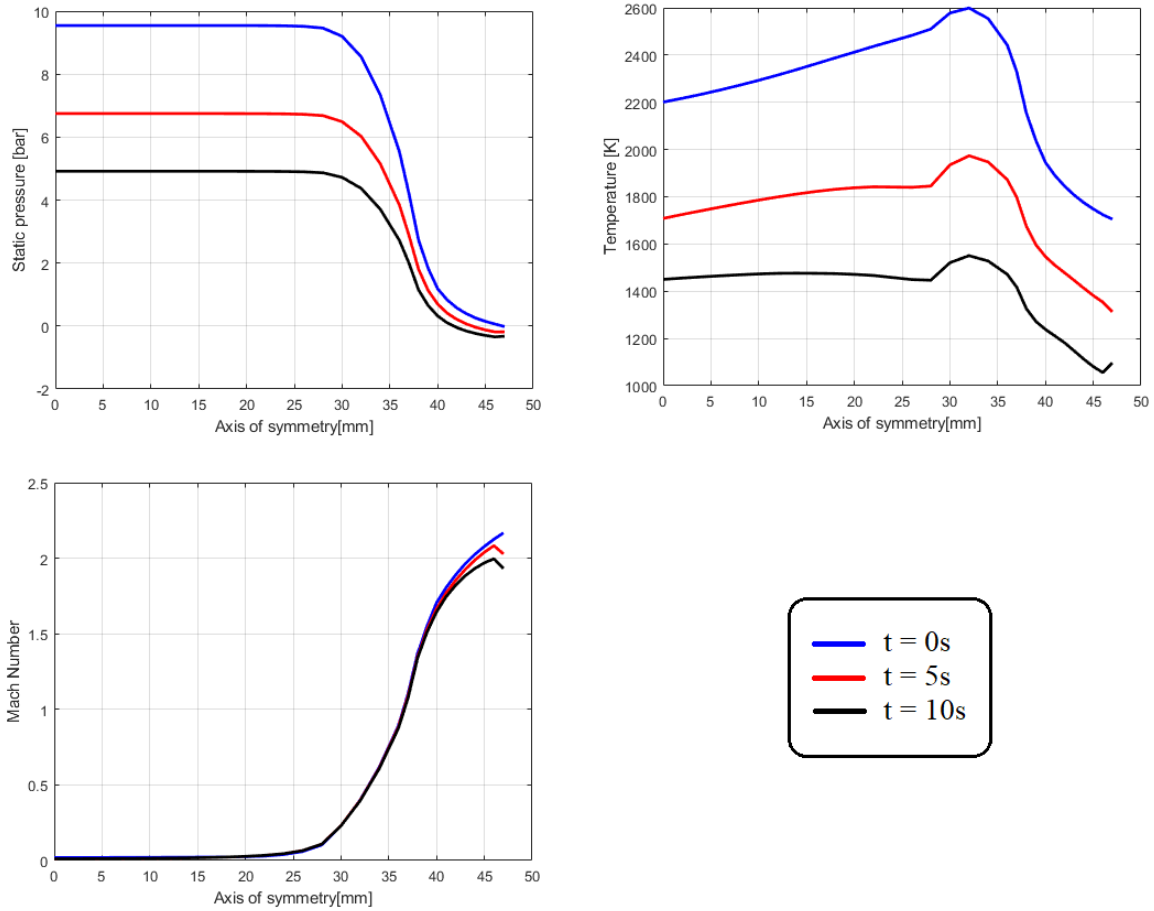

Figure 7. Area-weighted average of the properties pressure, temperature and Mach number along the nozzle.

the combustion port, increasing the volume of the flux during the propulsion process. Moreover, in the divergent part of the nozzle, the pressure and temperature decrease, and the velocity increase over time according to the theory of compressible flow, Anderson Jr (2011). However, the pressure damping inside the combustion chamber during the experimental tests may happen, but those values won't decrease as quickly as the values presented in Figure 7.

An analysis of the species inside the control volume was made to check the completeness of combustion at the initial time (t= 0s). In Figure 8 shows the distribution of O_2 and the mean mixture fraction. The consumption of O_2 through the fuel port up to the beginning of the post chamber is notable, as its mass fraction diminishes up to 40 % at the core of the nozzle. The mean mixture fraction is "1" where there is 100 % fuel or $nC_{16}H_{34}$, and "0" to oxygen. Therefore, Figure 8 presents a mixture of fuel and oxygen all over the post chamber and nozzle. Moreover, the big molecule of $nC_{16}H_{34}$ breaks rapidly into small molecules since there is a discrete red line close to the paraffin inlet. Those small molecules react in the post-chamber and near the nozzle's wall generating a high concentration of CO.

Figure 9 presents the distribution of some products of the combustion of Paraffin with oxygen, which are CO_2 and H_2O. CO_2 presents a concentration of around 6 % at the post chamber, between 5.5 % and 11 % near the nozzle's wall and between 22 % and 25 % at the core of the motor. H_2O shows lower values at the core of the motor of around 13 %, with values up to 20 % near the nozzle's wall, and between 8 % to 13 % at the post chamber. Therefore one can say that they summat up to 20 % at the post-chamber, 30 % near the nozzle's wall, and 38 % at the core of the motor.

The major part of the products of the combustion of $nC_{16}H_{34}$ with O_2 is CO since the O/F ratio is around 2.33 and the stoichiometric O/F is around 3.46. Therefore it presents poor oxygen combustion, and consequently, there is a higher concentration of CO since there was not enough oxygen to oxidize CO to CO_2. Figure 10 presents a CO mass fraction concentration of around 77 % at the post chamber, 70 % near the nozzle's wall, and between 7 % and 15 % at the core of the motor.

Therefore here was presented a simulation of the combustion inside the HRM. It was possible to evaluate the effects of the geometry of the parabolic nozzle on the gaseous expansion on the divergent part. The conclusion made in the first part is that the nozzle is adapted to a combustion chamber pressure of 10 bar. Lastly, the species distributions inside the motor were investigated, showing the distribution of O_2, CO_2, H_2O, CO and mean mixture fraction.

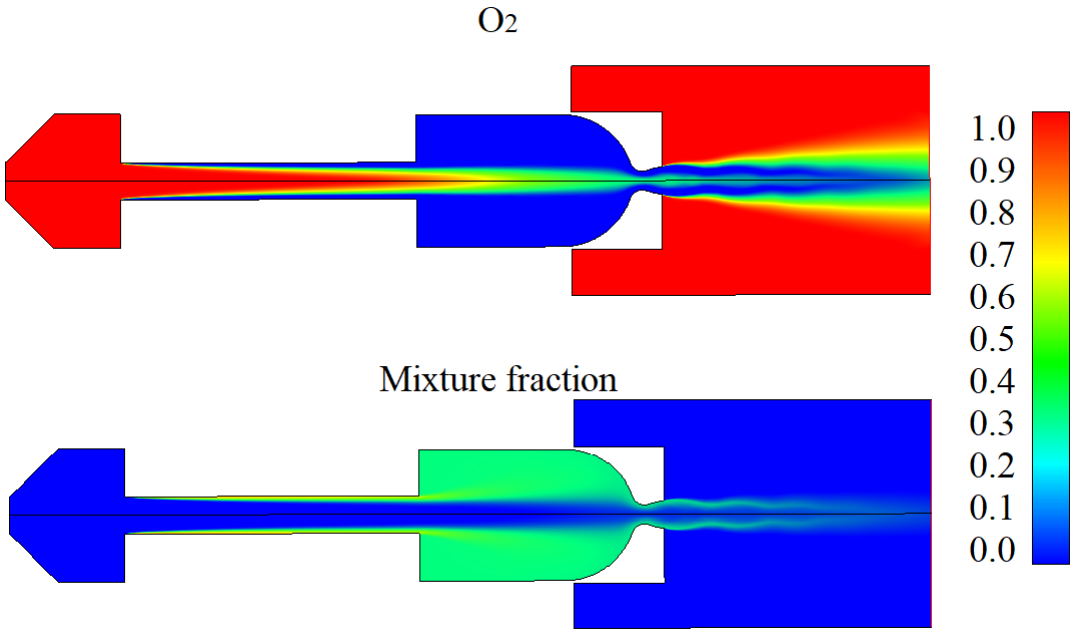

Figure 8. An area-weighted average of the specie O_2 and the mean mixture fraction along with the nozzle.

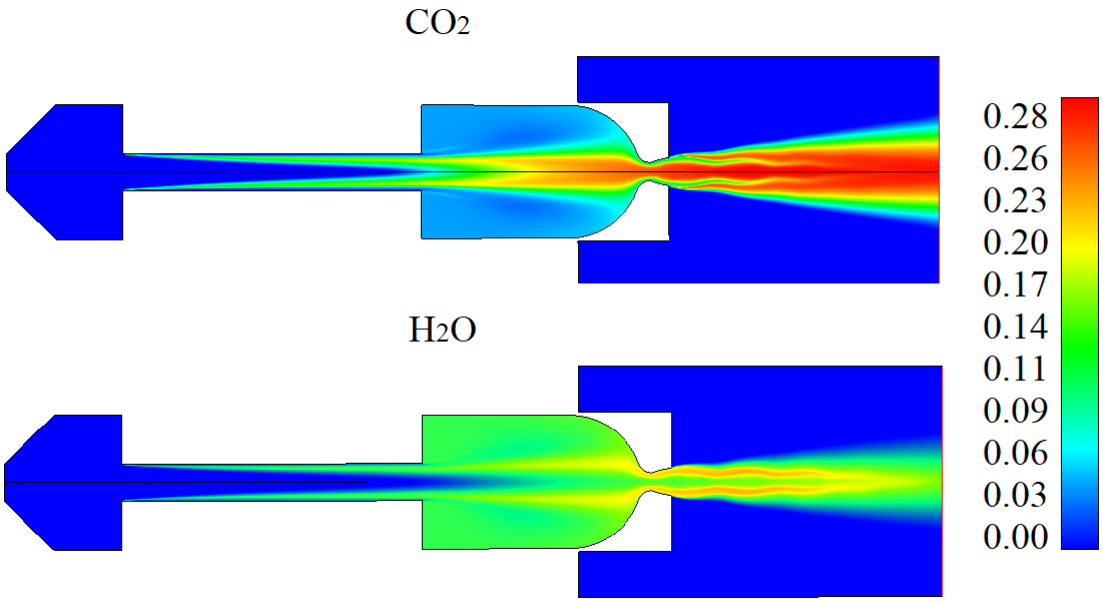

Figure 9. An area-weighted average the species CO_2 and H_2O along with the nozzle.

5. CONCLUSIONS and DISCUSSION:

The present work has presented a combustion simulation of paraffin with gaseous oxygen inside a hybrid rocket motor. Paraffin was treated as gaseous hexadecane $C_{16}H_{34}$ to avoid multiphase flows but still considering a higher alkane molecule to better represent the paraffin combustion. A detailed analytical part presented some theoretical results about the regression rate of paraffin as fuel and gaseous oxygen as the oxidizer. These results served as input into the simulations. With this simulation, it was possible to evaluate the flow properties inside the hybrid rocket motor and nozzle, such as pressure, temperature, and velocity.

The pressure drop inside the combustion chamber over time is due to the volume expansion of the port. However, this may happen during experimentation, and the pressure damping rate in the simulation was evaluated as unrealistic. Moreover, the nozzle was evaluated as approximately adapted and slightly over-expanded due to the pressure drop. The simulation results helped to improve the quality of the project of a hybrid rocket motor of 100 newtons.

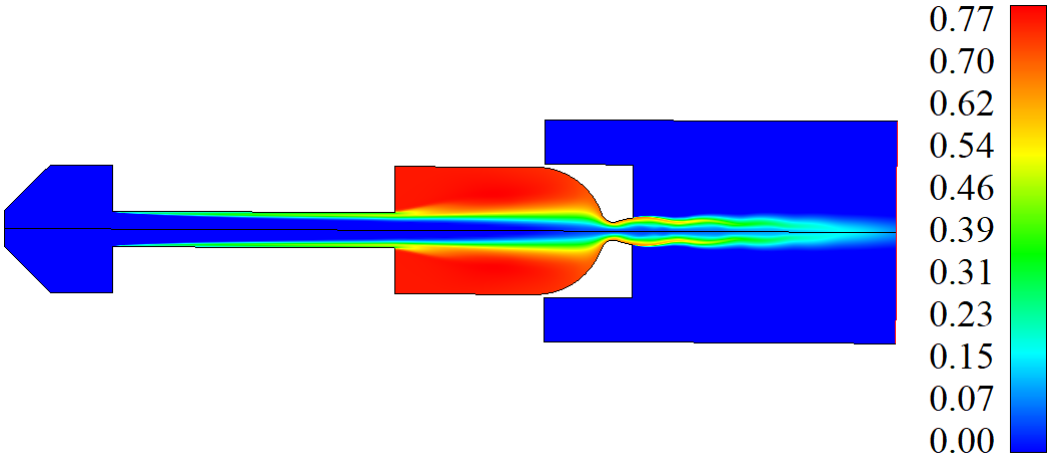

Figure 10. An area-weighted average the species *CO* along with the nozzle.

6. ACKNOWLEDGEMENTS

My thanks to CAPES for their financial support. The authors would like to acknowledge the financial support of ITAEx (project number 192027) and CNPq (project numbers 428039/2018-9, 432410/2018-0, and 406726/2018-3).

7. REFERENCES

Anderson Jr, J.D., 2011. *Fundamentals of aerodynamics*. Tata McGraw-Hill Education, 5th edition.

Ansys, 2006a. "Modeling turbulent flows". Introductory FLUENT Notes. 07 July 2018 <http://www.fluentusers.com>.

Ansys, 2006b. "Reynolds (ensemble) averaging". Fluent 6.3 User's Guide, section 12.2.2.

Ansys, 2006c. "Wall boundary conditions". Fluent 6.3 User's Guide, section 12.5.3.

ANSYS, 2009. "The model fluid81 implemented in ansys fluent". Theory Reference for the Mechanical APDL and Mechanical Applications, section 14.81.

Esch, T. and Menter, F., 2003. "Heat transfer prediction based on two-equation turbulence models with advanced wall treatment". *Turbulence Heat an Mass Transfer 4*.

Gordon, S. and J. McBride, B., 1994. "Computer program for calculation of complex chemical equilibrium compositions and applications. NASA RP-1311".

Humble, R.W., Henry, G.N. and Larson, W.J., 1995. "Hybrid rocket propulsion systems". In *Space Propulsion Analysis and Design*, McGraw-Hill Companies, New York, Vol. 1, pp. 365–441. ISBN 9780070313200.

Jones, W P; Launder, B.E., 1972. "The Prediction of Laminarization with a Two-Equation Model of Turbulence". *International Journal of Heat and Mass Transfer*, Vol. 15, pp. 301–314.

Karabeyoglu, M., Cantwell, B. and Altman, D., 2001. "Development and testing of paraffin-based hybrid rocket fuels". *AIAA 2001-4503. 37th Joint Propulsion Conference and Exhibit*. doi:10.2514/6.2001-4503.

Martino, G.D.D., Mungiguerra, S., Carmicino, C. and Savino, R., 2019. "Computational Fluid-Dynamic Modeling of the Internal Ballistics of Paraffin-Fueled Hybrid Rocket". *Aerospace Science and Technology*. ISSN 1270-9638. doi:10.1016/j.ast.2019.04.019.

Martins, P.G.C., de Souza, K.M. and de Lemos, M., 2019. "Numerical Study of Rugosity Effects in a Sinusoidal Pipe by Apllying k-Omega SST Turbulence Model." *25th International Congress of Mechanical Engineering*, pp. COB–2019–0963. doi:10.26678/ABCM.COBEM2019.COB2019-0963.

Martins, P.G.C. and Shynkarenko, O., 2017. " Flow Analysis Inside the Combustion Chamber and the Nozzle of a Hybrid Rocket Motor". *25th International Congress of Mechanical Engineering*, pp. COB–2017–0990. doi: 10.26678/ABCM.COBEM2017.COB17-0990.

Martins, P.G.C., de Souza, K.M., Boschi, R.F., Gouvêa, L.H. and Martins, C.A., 2022. "Design of injector plates for hybrid rocket motors test bench with gaseous oxygen". *CILAMCE, Proceedings of the XLIII Ibero-Latin-American Congress on Computational Methods in Engineering, ABMEC*, pp. 1–9. ISSN 2675-6269.

Martins, P.G.C., de Souza, K.M., Boschi, R.F., Gouvêa, L.H. and Martins, C.A., 2023. "Performance comparison of paraffin/ethanol fuel blends in a laboratory-scale hybrid rocket motor". *Journal of Propulsion and Power*, pp. 1–13. doi:10.2514/1.B39051.

Martins, P.G.C., 2018. *Design of a paraffin/Gox lab-scale hybrid rocket motor*. Dissertation, Aeronautics Institute of Technology, São José dos Campos.

Menter, F.R., 1994. "Two-equation eddy-viscosity turbulence models for engineering applications". *AIAA Journal*, Vol. 32,

No. 8, pp. 1598–1605. ISSN 0001-1452. doi:10.2514/3.12149.

Menter, F.R., Kuntz, M. and Langtry, R., 2003. "Ten Years of Industrial Experience with the SST Turbulence Model". *Turbulence Heat and Mass Transfer 4*, Vol. 4, pp. 625–632. ISSN 1662-8985. doi:10.4028/www.scientific.net/AMR.576.60.

Stagni, A., Frassoldati, A., Cuoci, A. and Ranzi, E., 2015. "Skeletal mechanism reduction through species-targeted sensitivity analysis Skeletal mechanism reduction through species-targeted sensitivity analysis ." , No. November. doi:10.1016/j.combustflame.2015.10.013.

Wilcox, D., 1993. *Turbulence modeling for CFD*. ISBN 0963605100. doi:0963605151.

8. RESPONSIBILITY NOTICE

The authors are solely responsible for the printed material included in this paper.